Relaxation to Negative Temperatures in Double Domain Systems

Yusuke Hama,[1,*] William J. Munro,[2,1] and Kae Nemoto[1]
[1]National Institute of Informatics, 2-1-2 Hitotsubashi, Chiyoda-ku, Tokyo 101-8430, Japan
[2]NTT Basic Research Laboratories, NTT Corporation, 3-1 Morinosato-Wakamiya, Atsugi-shi, Kanagawa 243-0198, Japan

(Received 30 December 2016; published 8 February 2018)

The engineering of quantum systems and their environments has led to our ability now to design composite or complex systems with the properties one desires. In fact, this allows us to couple two or more distinct systems to the same environment where potentially unusual behavior and dynamics can be exhibited. In this Letter we investigate the relaxation of two giant spins or collective spin ensembles individually coupled to the same reservoir. We find that, depending on the configuration of the two individual spin ensembles, the steady state of the composite system does not necessarily reach the ground state of the individual systems, unlike what one would expect for independent environments. Further, when the size of one individual spin ensemble is much larger than the second, collective relaxation can drive the second system to an excited steady state even when it starts in the ground state; that is, the second spin ensemble relaxes towards a negative-temperature steady state.

DOI: 10.1103/PhysRevLett.120.060403

In recent years, the hybridization of quantum systems has become a key technique to design and demonstrate novel quantum behaviors [1–4]. With the rapid progress in quantum coherent manipulation, hybrid quantum systems have now entered the regime where we can observe unexpected or rather counterintuitive behavior even in the presence of imperfections and noise [5–8]. Such hybrid systems have not only shown the capability to achieve superior properties each individual system alone cannot achieve [4,6,9], but they also shed light on the fundamental complexity of such quantum systems including coupling structures and decoherence mechanisms [10]. Currently, a number of such hybrid systems have been proposed (and realized in some cases) with various elements coming from atomic molecular and optical systems to solid-state systems including, for instance, trapped ions [11], optical or microwave cavities and resonators [12,13], electron and nuclear spin ensembles in quantum dots (QD) or nitrogen-vacancy (NV^-) centers in diamond [14–16], superconducting circuits in quantum electrodynamic systems [2,3], and mechanical resonators [16,17]. This large diversity of component systems really allows one to explore the unique space hybridization potentially allows. Typically, however, the focus has been on designing composite systems with superior properties. Our focus here is on the other regime of engineering such systems to explore unexpected and counterintuitive behavior. Examples include the superradiant decay of a spin ensemble collectively coupled with an optical mode [18,19] or spin ensemble squeezing via collective decoherence [20]. When those spins couple collectively with a bosonic reservoir, the spin dynamics dramatically changes from those driven by individual spin-boson coupling.

Typically investigations of such collective behavior have focused on single spin ensembles, primarily as they are experimentally easier to realize; however, multiple ensembles have the potential for quite counterintuitive behavior due to the complexity of the overall hybrid system [21]. Recently, several examples have been found experimentally to investigate this problem in the quantum Hall (QH) regime, the double nuclear spin domain formation generated by the dynamic nuclear polarization (DNP) [22,23], and the nuclear spin relaxation measurement where nuclear spin ensemble couples to the Nambu-Goldstone (NG) mode which may act as a bosonic reservoir [24,25].

In this Letter, we will model these experimental systems and explore a hybrid system composed of two giant spins or collective spin ensembles coupled to the same bosonic reservoir. These giant spins or spin ensembles may be part of the same physical system, so let us introduce some domainlike notation [26]. Spin domains allow one to partition an ensemble into distinct noninteracting components that yet still couple to the same bosonic reservoir. Our illustrative hybrid system example is schematically depicted in Fig. 1 as an ensemble of spin-$1/2$ particles coupled to a single bosonic reservoir. The ensemble is decomposed into two independent domains, each characterized by its initial state. Here we will focus on the dynamics of a double (sub)domain system; however, it is worth mentioning that the analysis can be easily expanded to multi-sub-domain systems. We will demonstrate that the dynamics of these two subdomains exhibit collective quantum phenomena such as superradiant decay. Further we will show that collective relaxation of the total system allows a subdomain to become excited even if it was initially in its ground state.

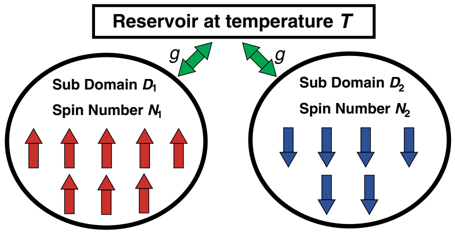

FIG. 1. Schematic representation of a double spin subdomain system coupled to a single reservoir. The double spin subdomain system may be formed from spin ensembles or giant spins. Here we denote the first spin subdomain D_1 containing N_1 spins shown as red arrows, while the second spin domain D_2 contains N_2 spins represented by blue arrows. In both subdomains, each spin couples with the bosonic reservoir (at a temperature T) with coupling constant g.

Let us now turn our attention to a mathematical description of our hybrid system where our total ensemble (as shown in Fig. 1) is divided into two spin subdomains labeled as domain D_1 and D_2. Each domain $D_{1(2)}$ contains $N_{1(2)}$ 1/2 spins with the same energy $\hbar\omega_s$. For descriptive convenience we will assume that all spins in a subdomain are initially aligned in the same direction (either upwards or downwards along the z axis). This in turn means that each subdomain starts off in a symmetric state; however, the overall system is not in the symmetric state (unless all spins in the total system align in the same direction). We can regard the subdomain $D_{1(2)}$ as a collective spin $J_{1(2)}$ whose spin magnitude is $N_{1(2)}/2$. Next, the spins in the subdomains D_1 and D_2 couple with the bosonic reservoir with a coupling constant $g \ll \omega_s$. Our overall system composed of two subdomains and the reservoir can then be desribed by the Hamiltonian

$$H = \hbar\omega_s(J_1^z + J_2^z) + \int d^d k E_{\boldsymbol{k}} r_{\boldsymbol{k}}^\dagger r_{\boldsymbol{k}} + \frac{\hbar g}{2}[(J_1^+ + J_2^+)R + (J_1^- + J_2^-)R^\dagger], \quad (1)$$

where the first term represents the Hamiltonian of the two subdomains with $J_i^{x,y,z}$ being the usual x, y, z collective spin operators for the ith subdomain. The raising (lowering) operators of these collective spins are defined by $J_i^\pm = J_i^x \pm iJ_i^y$. The second term represents the Hamiltonian of the reservoir where $E_{\boldsymbol{k}}$ is the linear dispersion relation of the reservoir with $r_{\boldsymbol{k}}(r_{\boldsymbol{k}}^\dagger)$ the annihilation (creation) operator satisfying the commutation relation $[r_{\boldsymbol{k}}, r_{\boldsymbol{k}'}^\dagger] = \delta(\boldsymbol{k} - \boldsymbol{k}')$. d is the spatial dimension of the system, and $\boldsymbol{k} = (k_1, \ldots, k_d)$ the wave vector of the reservoir. The final Hamiltonian represents the interaction between the two domains and the reservoir with the coupling strength g, where $R = \int d^d k \kappa_{\boldsymbol{k}} r_{\boldsymbol{k}}$ with $\kappa_{\boldsymbol{k}}$ being a continuous function of $\boldsymbol{k}$ whose exact form depends on the system under consideration.

Using a second order perturbation approach we can derive a Lindblad master equation for the reduced density matrix composed only of the two domains defined by $\rho_S(t) = \mathrm{Tr}_R[W(t)]$ with $W(t)$ the density matrix for the total system and Tr_R representing the operation tracing out the reservoir degrees of freedom. Further, we assume that initially the spin subdomains and the reservoir are uncorrelated. We can then characterize the reservoir by the density matrix $\rho_R = \exp(-H_R/k_BT)/\mathrm{Tr}_R(\exp(-H_R/k_BT))$ with H_R being the second term in Eq. (1) while k_B is the Boltzmann constant and T the reservoir temperature. The master equation using the Born-Markov approximation can be written as [27]

$$\dot{\rho}_S(t) = -i\omega_s[J_1^z + J_2^z, \rho_S(t)] + \gamma(\bar{n}+1)\mathcal{L}(J_1^- + J_2^-) + \gamma\bar{n}\mathcal{L}(J_1^+ + J_2^+), \quad (2)$$

where $\mathcal{L}(A) = 2A\rho A^\dagger - A^\dagger A\rho - \rho A^\dagger A$, while $\bar{n} = 1/(e^{\hbar\omega_s/k_BT} - 1)$ is the Bose-Einstein distribution and γ is the damping rate that is a function of both the coupling g and $|\kappa_{\boldsymbol{k}}|^2$ at the wave vector $\boldsymbol{k}_s$ (satisfying $E_{\boldsymbol{k}_s} = \hbar\omega_s$). Now from (2) the equations of motion for the expectation values of collective spins can be expressed as

$$\begin{aligned}
\frac{d}{dt}\langle J_{1(2)}^z\rangle &= -2\gamma(2\bar{n}+1)\langle J_{1(2)}^z\rangle \\
&\quad + \frac{\gamma}{2}(-N_{1(2)}(N_{1(2)}+2) + 4\langle J_{1(2)}^z\rangle^2 - 2\langle A_{12}\rangle), \\
\frac{d}{dt}\langle A_{12}\rangle &= -2\gamma(2\bar{n}+1)(\langle A_{12}\rangle - 4\langle J_1^z J_2^z\rangle) \\
&\quad + 2\gamma(\langle J_1^z\rangle + \langle J_2^z\rangle)(\langle A_{12}\rangle - 2\langle J_1^z J_2^z\rangle) \\
&\quad + \gamma(N_2(N_2+2)\langle J_1^z\rangle + N_1(N_1+2)\langle J_2^z\rangle) \\
\frac{d}{dt}\langle J_1^z J_2^z\rangle &= -\frac{1}{2}\frac{d}{dt}\langle A_{12}\rangle,
\end{aligned} \quad (3)$$

with $A_{12} = J_1^+ J_2^- + J_1^- J_2^+$ representing spin flip flop between the two subdomains and where we have factorized moments [28] as

$$\begin{aligned}
&\langle (J_i^z)^2\rangle \approx \langle J_i^z\rangle^2, \qquad \langle J_i^z (J_j^z)^2\rangle \approx \langle J_i^z J_j^z\rangle\langle J_j^z\rangle, \\
&\langle J_i^z J_i^\pm J_j^\mp\rangle \approx \langle J_i^\pm J_j^\mp\rangle\langle J_i^z\rangle \pm \langle J_i^\pm J_j^\mp\rangle, \\
&\langle J_i^\pm J_i^z J_j^\mp\rangle \approx \langle J_i^\pm J_j^\mp\rangle\langle J_i^z\rangle,
\end{aligned} \quad (4)$$

with i, $j = 1, 2$ ($i \neq j$). The collective spin relaxations in the double spin domain system are described by four dynamical variables: $\langle J_1^z\rangle$, $\langle J_2^z\rangle$, $\langle J_1^z J_2^z\rangle$, and $\langle A_{12}\rangle$. The spin flip-flop $\langle A_{12}\rangle$ dynamics may be identified with that of the correlation between the J_1^z and J_2^z as seen from Eq. (3).

Let us now investigate the relaxation processes under the various conditions in terms of the initial spin-domain configuration and domain numbers N_1 and N_2. We show the effect of such processes in Figs. 2–5 where

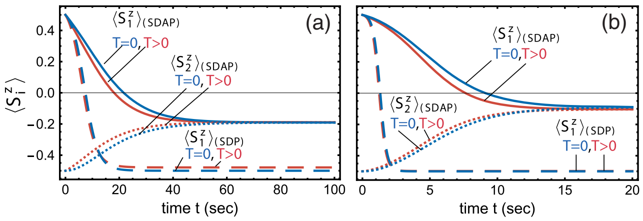

FIG. 2. Plot of the normalized collective spin relaxations for balanced number configurations. (a) $N_1 = N_2 = 10$ and (b) $N_1 = N_2 = 100$. The blue (red) curves are for $T = 0$ K (400 mK). The solid (dotted) curves represent $\langle S_1^z \rangle$ ($\langle S_2^z \rangle$) under the initial condition $|\mathrm{SDAP}\rangle$, while the dashed curves are the relaxations under the condition $|\mathrm{SDP}\rangle$. We have chosen $\omega_s/2\pi = 10$ GHz with $\gamma = 0.01$ Hz.

relaxations are described by the normalized spin $\langle S_{1(2)}^z \rangle = \langle J_{1(2)}^z \rangle / N_{1(2)}$. For an initial state, we take the antiparallel configuration

$$|\mathrm{SDAP}\rangle = |\uparrow \ldots \uparrow\rangle_{D_1} \otimes |\downarrow \ldots \downarrow\rangle_{D_2}. \qquad (5)$$

An example of this initial spin state is the double nuclear spin domains in the QH system which is realized by the DNP [22,23]. To understand the essence of this spin relaxation process more clearly, we focus on the steady state behavior and the relaxation times for each domain. In the case of the balanced system, that is, domains of equal spin size, the results shown in Fig. 2 indicate that starting with the antiparallel configuration (5) the relaxation process for each domain is similar, decaying to the steady state with the same $\langle S_i^z \rangle$ ($i = 1, 2$). The average number of excitations at the steady state is dependent on both the domain size N_i and, of course, the reservoir temperature. Here, the blue curves are the relaxation processes for the zero temperature while red curves are those for finite temperature.

As a comparison, the dashed curves show the decay process under the parallel configuration initial state defined by

$$|\mathrm{SDP}\rangle = |\uparrow \ldots \uparrow\rangle_{D_1} \otimes |\uparrow \ldots \uparrow\rangle_{D_2}. \qquad (6)$$

As both this initial state (6) and the Hamiltonian (1) satisfy the symmetry of SU(2) for the total collective spin, the total state decays on the symmetric subspace. In this case, the collective effect of the decay, i.e., superradiant, is most prominent. This superradiant effect becomes more visible as the spin size increases as we illustrate in Fig. 2 for (a) $N_1 = N_2 = 10$ and (b) $N_1 = N_2 = 100$ (The finite temperature relaxation shows a similar behavior). To illustrate the dependency of the relaxation time τ_N for the antiparallel configuration (5) on the subdomain size, we plot τ_N in Fig. 3 versus $N = N_1 = N_2$ for both zero temperature and 400 mK. Here we identify τ_N with the time when $\langle J_{1(2)}^z \rangle$ becomes $e \sim 2.718$ times smaller than the

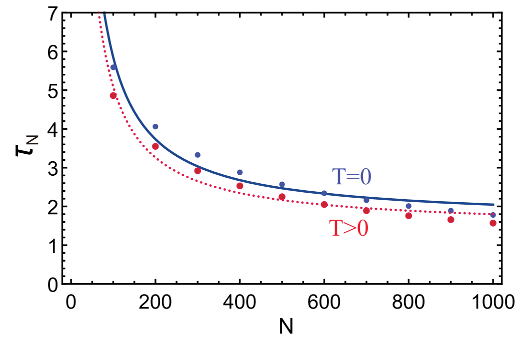

FIG. 3. Plot of the relaxation time τ_N for the initial configuration $|\mathrm{SDAP}\rangle$ as a function of subdomain size N for zero temperature (blue solid line) and finite (400 mK) temperature (red dotted line). Curve fitting indicates a functional form for $\tau_N \sim a/N + b$ with $a = 422.33$, $b = 1.62$ for $T = 0$ and $a = 365.64$, $b = 1.43$ for $T > 0$. The $1/N$ dependence is a clear signature of superradiant decay [19].

expectation value of $J_{1(2)}^z$ (or $\langle S_{1(2)}^z \rangle$) at initial time. Curve fitting to these data points shows τ_N has the form $a/N + b$, a clear signature of superradiant decay [19].

The steady state of the antiparallel configuration for each domain contains more excitations than the parallel configuration case. This is due to the smaller spin size for each domain ($N_{1,2} < N_1 + N_2$) and the violation of the SU(2) symmetry at the initial time of the dynamics. We can always write the antiparallel configuration as a sum of a symmetric subspace component and a nonsymmetric subspace component. The symmetric subspace component decays like in the parallel configuration case; however, the nonsymmetric subspace component decays differently. This will be illustrated in more detail next when we discuss the unbalanced case $N_1 \neq N_2$.

In Fig. 4 we plot $\langle S_1^z \rangle$ (red solid line), $\langle S_2^z \rangle$ (blue dot line), and $\langle S^z \rangle = (\langle J_1^z \rangle + \langle J_2^z \rangle)/(N_1 + N_2)$ (green dash line) for various unbalanced configuration $N_1 > N_2$ with $N_1 = 2, 5$ and $N_2 = 1$ at zero temperature (the 400 mK situation which is not shown displays similar characteristics).

In these unbalanced spin size cases, the smallest domain D_2 shows completely different relaxation compared to the

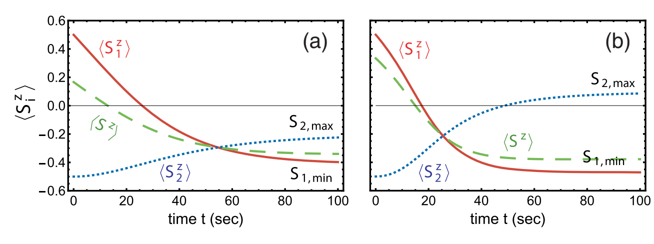

FIG. 4. Plot of the collective spin relaxations for various unbalanced number configurations ($N_1 > N_2$) at zero temperature. The configuration considered are (a) $N_1 = 2$, $N_2 = 1$ and (b) $N_1 = 5$, $N_2 = 1$. The red solid curves, blue dotted curves, and green dashed curves represent $\langle S_1^z \rangle$, $\langle S_2^z \rangle$, and $\langle S^z \rangle$, respectively. $S_{1,\mathrm{min}}^z$ ($S_{2,\mathrm{max}}^z$) are the steady-state solution for $\langle S_{1(2)}^z \rangle$.

larger domain D_1. In fact, although D_2 was initialized in the ground state of the domain as given by Eq. (5), this subsystem relaxed into more highly excited states (even at zero temperature). More interestingly, (b) for $N_1 = 5$, $N_2 = 1$ show that the second domain decays to a steady state the population of spins in the excited state is greater than 50%. In fact, the steady state of the second domain at zero temperature for $N_1 = N$, $N_2 = 1$ scales as

$$\langle J_2^z \rangle \sim \frac{(N-1)^2 - 2}{2(N+1)^2}, \tag{7}$$

and gradually gets closer to an almost fully excited state when the system size gets larger. This behavior is not restricted to $N_2 = 1$ and so to illustrate this point further, we plot in Fig. 5 the relaxation process for $N_1 = 10^4$ with $N_2 = 10^2$ again at zero temperature. It can be clearly seen that in the steady state the second domain is approaching the fully excited state, despite superradiant relaxation of the first domain leading it to its ground state with $\langle J_1^z \rangle \sim -N_1/2$.

As a result, when the first domain spin size is sufficiently larger than the second one, the second domain relaxes to the steady state where the spin population in the excited state is greater than 50%, i.e., the negative temperature state. So far we have assumed equal coupling strengths between the each spin and reservoir [see Eq. (1)] but this is not necessary. Unequal coupling between the two domains and the bosonic reservoir also leads to the negative temperature phenomena in quite general cases [29].

Let us explore this decay characteristics of the collective coupling through the example $N_1 = 5$, $N_2 = 1$, which is shown in Fig. 4(b). With an initial state $|\uparrow_1 \ldots \uparrow_5\rangle_{D_1} \otimes |\downarrow_6\rangle_{D_2}$, we need to consider two manifolds of the total system: that is, the symmetric subspace of the spin size $(N_1 + N_2)/2$ and the second subspace of the spin size $(N_1 + N_2 - 2)/2$. The dynamics conserves the spin size, these two subspaces are enough to represent the total system through the entire dynamics, and there is no transfer of the population between these subspaces. The initial component in each manifold decays via the coupling to the reservoir; hence, the component on the symmetric manifold will decay to the ground state $|\downarrow_1 \ldots \downarrow_6\rangle$. Similarly, the component on the second manifold will decay to its ground state. The decay process is confined in each subspace and hence gives the steady states the excitations in the second domain. The decay to a negative temperature is not due to the energy flow from the first domain to the second domain via the reservoir, because an energy exchange occurs only between the reservoir and the double domains. Therefore, this behavior must be a result of the collective decay of the total spin system. This mechanism of collective decay also may generate entanglement between the two domains at the steady state, even though the initial state is separable.

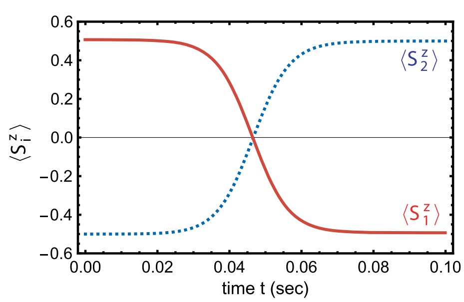

FIG. 5. Plot of the normalized collective spin relaxations $\langle S_1^z \rangle$ (red solid line) and $\langle S_2^z \rangle$ (blue dot line) for the unbalanced configuration at zero temperature. Here we take $N_1 = 10^4$ and $N_2 = 10^2$.

Next we turn our attention to potential physical systems which may be able to realize our collective spin relaxations. Two types of physical systems come to our attention with the first being a hybrid system of electron and nuclear spins in GaAs semiconductors [14,22–25,30–33]. As mentioned before, when this system is set into the quantum Hall regime, the double nuclear spin domains can be created by initially polarizing the nuclear spin ensemble via DNP [22,23,30–32,34]. Then, coupling them to the NG mode the negative temperature relaxation should be observed. The second potential system is electron spin ensembles formed from NV^- centers in diamond coupled to superconducting resonators [21]. Here the two electron spin ensembles can be coupled jointly to the superconducting resonators opening the possibility for negative temperature experiments in this regime. In the actual systems, however, there are many error sources, for instance, the dephasing effects, which destroy the collective phenomena. We have not included such effects since our interest was the spin collective dynamics. Even though it is included, we should observe our spin collective phenomena by focusing on the dynamics on a time scale shorter than the spin dephasing time. This is because as we see in Figs. 2–5 the relaxation time for the collective phenomena depends on the spin sizes and for large domains it is shorter than the spin dephasing time.

Usually we assume ancillary systems coupled only to the reservoir can be ignored; however, as our analysis has shown, when there are other systems coupled to the same reservoir, they can affect the system of interest significantly. Even when the temperature of the shared reservoir is fixed, one needs to be careful to define temperature for the system at hand, as the temperature of each domain appears to be different. These effects are much more prominent with the shared reservoir in comparison to the dynamics seen in the systems coupled with independent reservoirs.

The negative-temperature relaxation presented in our Letter is due to the collective behaviors of the two spin ensembles. On the other hand, in Ref. [35] it has been shown that the negative-temperature state was experimentally realized using the LiF crystal, and theoretically investigated in Ref. [36] in terms of an entropy argument (other theoretical studies and experimental setups for such negative-temperature state realization, see references therein). The negative-temperature states shown in these references are driven not by the collective phenomena but by the inversion of the external parameter such as the sign of the external magnetic field. Furthermore, our negative-temperature behavior occurs even when the reservoir temperature approaches zero, which is not the case for the systems shown in Refs. [35,36].

To summarize, we have investigated in this Letter collective spin relaxation processes in a double spin-domain system where all spins in the two domains are collectively coupled to a single bosonic reservoir. The dynamics of the total system, of course, shows superradiant decay but also shows excitations arising in one of the domains initially prepared in its ground state, even for a zero temperature reservoir with no direct coupling between domains. In fact, when there is a large imbalance in the size or number of spins in each domain we can see the relaxation to a negative temperature in the smaller one. This decay behavior appears more prominent as the domain size difference increases.

We thank Mohammad Hamzah Fauzi, Yoshiro Hirayama, and Emi Yukawa for fruitful discussions and comments. This work was supported in part by the RIKEN Special Postdoctoral Researcher Program (Y. H.) and the MEXT KAKENHI Grant No. 15H05870 (K. N. and Y. H.).

*yskhama@nii.ac.jp

[1] M. Wallquist, K. Hammerer, P. Rabl, M. Lukin, and P. Zoller, Hybrid quantum devices and quantum engineering, Phys. Scr. **T137**, 014001 (2009).

[2] Z.-L. Xiang, S. Ashhab, J. Q. You, and F. Nori, Hybrid quantum circuits: Superconducting circuits interacting with other quantum systems, Rev. Mod. Phys. **85**, 623 (2013).

[3] G. Kurizki, P. Bertet, Y. Kubo, K. Mølmer, D. Petrosyan, P. Rabl, and J. Schmiedmayer, Quantum technologies with hybrid systems, Proc. Natl. Acad. Sci. U.S.A. **112**, 3866 (2015).

[4] S. Putz, A. Angerer, D. O. Krimer, R. Glattauer, W. J. Munro, S. Rotter, J. Schmiedmayer, and J. Majer, Spectral hole burning and its application in microwave photonics, Nat. Photonics **11**, 36 (2017).

[5] T. Langen, T. Gasenzer, and J. Schmiedmayer, Prethermalization and universal dynamics in near-integrable quantum systems, J. Stat. Mech. (2016) 064009.

[6] Y. Matsuzaki, X. Zhu, K. Kakuyanagi, H. Toida, T. Shimo-Oka, N. Mizuochi, K. Nemoto, K. Semba, W. J. Munro, H. Yamaguchi, and S. Saito, Improving the Coherence Time of a Quantum System via a Coupling to a Short-Lived System, Phys. Rev. Lett. **114**, 120501 (2015).

[7] P. Forn-Díaz, J. J. García-Ripoll, B. Peropadre, J.-L. Orgiazzi, M. A. Yurtalan, R. Belyansky, C. M. Wilson, and A. Lupascu, Ultrastrong coupling of a single artificial atom to an electromagnetic continuum in the nonperturbative regime, Nat. Phys. **13**, 39 (2017).

[8] F. Yoshihara, T. Fuse, S. Ashhab, K. Kakuyanagi, S. Saito, and K. Semba, Superconducting qubit-oscillator circuit beyond the ultrastrong-coupling regime, Nat. Phys. **13**, 44 (2017).

[9] K. Nemoto and W. J. Munro, Universal quantum computation on the power of quantum non-demolition measurements, Phys. Lett. A **344**, 104 (2005).

[10] J. Jeske, N. Vogt, and J. H. Cole, Excitation and state transfer through spin chains in the presence of spatially correlated noise, Phys. Rev. A **88**, 062333 (2013).

[11] D. Leibfried, R. Blatt, C. Monroe, and D. Wineland, Quantum dynamics of single trapped ions, Rev. Mod. Phys. **75**, 281 (2003).

[12] J. M. Raimond, M. Brune, and S. Haroche, Manipulating quantum entanglement with atoms and photons in a cavity, Rev. Mod. Phys. **73**, 565 (2001).

[13] H. Ritsch, P. Domokos, F. Brennecke, and T. Esslinger, Cold atoms in cavity-generated dynamical optical potentials, Rev. Mod. Phys. **85**, 553 (2013).

[14] R. Hanson, L. P. Kouwenhoven, J. R. Petta, S. Tarucha, and L. M. K. Vandersypen, Spins in few-electron quantum dots, Rev. Mod. Phys. **79**, 1217 (2007).

[15] R. Schirhagl, K. Chang, M. Loretz, and C. L. Degen, Nitrogen-vacancy centers in diamond: nanoscale sensors for physics and biology, Annu. Rev. Phys. Chem. **65**, 83 (2014).

[16] D. Lee, K. W. Lee, J. V. Cady, P. Ovartchaiyapong, and A. C. Bleszynski Jayich, Topical review: spins and mechanics in diamond, J. Opt. **19**, 033001 (2017).

[17] M. Aspelmeyer, T. J. Kippenberg, and F. Marquardt, Cavity optomechanics, Rev. Mod. Phys. **86**, 1391 (2014).

[18] R. H. Dicke, Coherence in spontaneous radiation processes, Phys. Rev. **93**, 99 (1954).

[19] M. Gross and S. Haroche, Superradiance: An essay on the theory of collective spontaneous emission, Phys. Rep. **93**, 301 (1982).

[20] S. Dooley, E. Yukawa, Y. Matsuzaki, G. C. Knee, W. J. Munro, and K. Nemoto, A hybrid-systems approach to spin squeezing using a highly dissipative ancillary system, New J. Phys. **18**, 053011 (2016).

[21] T. Astner, S. Nevlacsil, N. Peterschofsky, A. Angerer, S. Rotter, S. Putz, J. Schmiedmayer, and J. Majer, Coherent Coupling of Remote Spin Ensembles via a Cavity Bus, Phys. Rev. Lett. **118**, 140502 (2017).

[22] M. H. Fauzi, S. Watanabe, N. Kumada, and Y. Hirayama, All electrical probe of nuclear spin polarization and relaxation by spin phase transition peaks of the filling fraction $\nu = 2/3$ quantum Hall effect, J. Korean Phys. Soc. **60**, 1676 (2012).

[23] M. H. Fauzi, S. Watanabe, and Y. Hirayama, Microscopic characteristics of dynamic nuclear polarization and selective nuclear depolarization at the $\nu = 2/3$ spin phase transition, Appl. Phys. Lett. **101**, 162105 (2012).

[24] N. Kumada, K. Muraki, and Y. Hirayama, Low-frequency spin dynamics in a canted antiferromagnet, Science **313**, 329 (2006); NMR Evidence for Spin Canting in a Bilayer $\nu = 2$ Quantum Hall System, Phys. Rev. Lett. **99**, 076805 (2007).

[25] M. H. Fauzi, S. Watanabe, and Y. Hirayama, Nuclear magnetometry studies of spin dynamics in quantum Hall systems, Phys. Rev. B **90**, 235308 (2014).

[26] The domain notation is commonly used in the solid-state community.

[27] H. J. Carmichael, *Statistical Methods in Quantum Optics 1: Master Equations and Fokker-Planck Equations*, 2nd ed. (Springer, Berlin, 2002).

[28] D. Meiser and M. J. Holland, Intensity fluctuations in steady-state superradiance, Phys. Rev. A **81**, 063827 (2010).

[29] An unbalanced coupling between the two spin ensembles and reservoir can be represented by a Hamiltonian of the form $(\hbar/2)(g_1 J_1^+ + g_2 J_2^+)R + \mathrm{H.c.}$. At zero temperature with $N_1 \gg N_2$, negative-temperature states can be realized even there is a moderate unbalance between g_1 and g_2. For instance, the negative temperature is seen for $N_1 = 4$ and $N_2 = 1$ with $g_2 = 1.5g_1$.

[30] W. A. Coish and J. Baugh, Nuclear spins in nanostructures, Phys. Status Solidi B **246**, 2203 (2009).

[31] Y. Hirayama, G. Yusa, K. Hashimoto, N. Kumada, T. Ota, and K. Muraki, Electron-spin/nuclear-spin interactions and NMR in semiconductors, Semicond. Sci. Technol. **24**, 023001 (2009).

[32] E. A. Chekhovich, M. N. Makhonin, A. I. Tartakovskii, A. Yacoby, H. Bluhm, K. C. Nowack, and L. M. K. Vandersypen, Nuclear spin effects in semiconductor quantum dots, Nat. Mater. **12**, 494 (2013).

[33] Y. Hama, M. H. Fauzi, K. Nemoto, Y. Hirayama, and Z. F. Ezawa, Dicke model for quantum Hall systems, New J. Phys. **18**, 023027 (2016).

[34] S. E. Economou and E. Barnes, Theory of dynamic nuclear polarization and feedback in quantum dots, Phys. Rev. B **89**, 165301 (2014).

[35] E. M. Purcell and R. V. Pound, A nuclear spin system at negative temperature, Phys. Rev. **81**, 279 (1951).

[36] E. Abraham and O. Penrose, Physics of negative absolute temperatures, Phys. Rev. E **95**, 012125 (2017).